



**HAL**  
open science

## **Stability of relativistic electron trapping by strong whistler or electromagnetic ion cyclotron waves**

A. V. Artemyev, D. Mourenas, O. V. Agapitov, D. L. Vainchtein, F. S. Mozer, V. Krasnoselskikh

### ► **To cite this version:**

A. V. Artemyev, D. Mourenas, O. V. Agapitov, D. L. Vainchtein, F. S. Mozer, et al.. Stability of relativistic electron trapping by strong whistler or electromagnetic ion cyclotron waves. *Physics of Plasmas*, 2015, 22 (8), 082901 (13 p.). <10.1063/1.4927774>. <insu-01280779>

**HAL Id: insu-01280779**

**<https://insu.hal.science/insu-01280779v1>**

Submitted on 1 Mar 2016

**HAL** is a multi-disciplinary open access archive for the deposit and dissemination of scientific research documents, whether they are published or not. The documents may come from teaching and research institutions in France or abroad, or from public or private research centers.

L'archive ouverte pluridisciplinaire **HAL**, est destinée au dépôt et à la diffusion de documents scientifiques de niveau recherche, publiés ou non, émanant des établissements d'enseignement et de recherche français ou étrangers, des laboratoires publics ou privés.



HAL Authorization

## Stability of relativistic electron trapping by strong whistler or electromagnetic ion cyclotron waves

A. V. Artemyev, D. Mourenas, O. V. Agapitov, D. L. Vainchtein, F. S. Mozer, and V. Krasnoselskikh

Citation: *Physics of Plasmas* **22**, 082901 (2015); doi: 10.1063/1.4927774

View online: <http://dx.doi.org/10.1063/1.4927774>

View Table of Contents: <http://scitation.aip.org/content/aip/journal/pop/22/8?ver=pdfcov>

Published by the **AIP Publishing**

---

### Articles you may be interested in

[Nonlinear electron acceleration by oblique whistler waves: Landau resonance vs. cyclotron resonance](#)  
*Phys. Plasmas* **20**, 122901 (2013); 10.1063/1.4836595

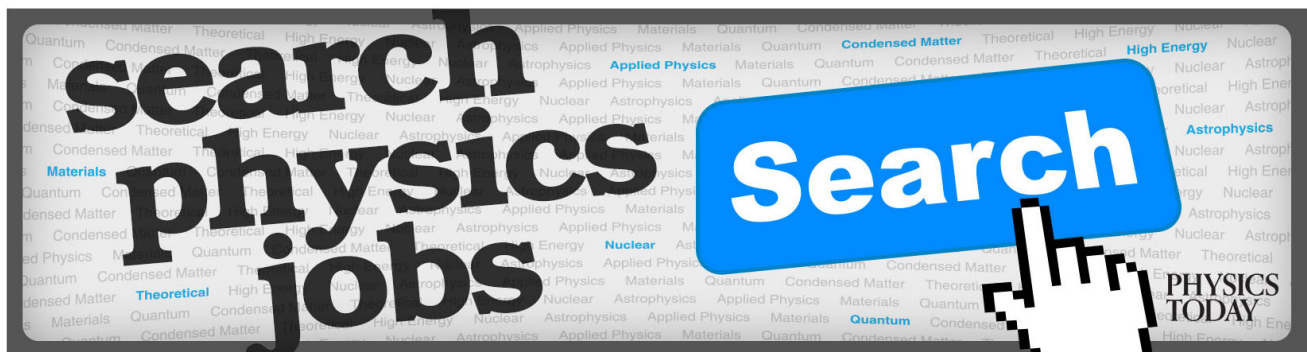
[Nonlinear electron motion in a coherent whistler wave packet](#)  
*Phys. Plasmas* **15**, 073506 (2008); 10.1063/1.2959121

[Precipitation of trapped relativistic electrons by amplified whistler waves in the magnetosphere](#)  
*Phys. Plasmas* **14**, 062903 (2007); 10.1063/1.2743618

[Computer simulations of relativistic whistler-mode wave–particle interactions](#)  
*Phys. Plasmas* **11**, 3530 (2004); 10.1063/1.1757457

[Pitch-angle diffusion of relativistic electrons due to resonant interactions with whistler waves](#)  
*Phys. Plasmas* **6**, 4597 (1999); 10.1063/1.873747

---



## Stability of relativistic electron trapping by strong whistler or electromagnetic ion cyclotron waves

A. V. Artemyev,<sup>1,2,a)</sup> D. Mourenas,<sup>3</sup> O. V. Agapitov,<sup>2,b)</sup> D. L. Vainchtein,<sup>4,c)</sup> F. S. Mozer,<sup>2</sup> and V. Krasnoselskikh<sup>1</sup>

<sup>1</sup>LPC2E/CNRS - University of Orleans, 3A Avenue de la Recherche Scientifique, F-45071 Orleans Cedex, France

<sup>2</sup>Space Sciences Laboratory, University of California, Berkeley, California 94720, USA

<sup>3</sup>CEA, DAM, DIF, F-91297 Arpajon Cedex, France

<sup>4</sup>Department of Mechanical Engineering, Temple University, Philadelphia, Pennsylvania 19122, USA

(Received 11 June 2015; accepted 9 July 2015; published online 13 August 2015)

In the present paper, we investigate the trapping of relativistic electrons by intense whistler-mode waves or electromagnetic ion cyclotron waves in the Earth's radiation belts. We consider the non-resonant impact of additional, lower amplitude magnetic field fluctuations on the stability of electron trapping. We show that such additional non-resonant fluctuations can break the adiabatic invariant corresponding to trapped electron oscillations in the effective wave potential. This destruction results in a diffusive escape of electrons from the trapped regime of motion and thus can lead to a significant reduction of the efficiency of electron acceleration. We demonstrate that when energetic electrons are trapped by intense parallel or very oblique whistler-mode waves, non-resonant magnetic field fluctuations in the whistler-mode frequency range with moderate amplitudes around 3 – 15 pT (much less intense than the primary waves) can totally disrupt the trapped motion. However, the trapping of relativistic electrons by electromagnetic ion cyclotron waves is noticeably more stable. We also discuss how the proposed approach can be used to estimate the effects of wave amplitude modulations on the motion of trapped particles. © 2015 AIP Publishing LLC. [<http://dx.doi.org/10.1063/1.4927774>]

### I. INTRODUCTION

Relativistic electron trapping (and/or phase bunching) by strong electromagnetic whistler or ion cyclotron (EMIC) waves is believed to play an important role in the formation of small populations of high-energy particles in the Earth's radiation belts<sup>9,16,18,20,54</sup> as well as in bursty precipitations of electrons into the atmosphere.<sup>32,49,59,78</sup> Moreover, nonlinear wave-particle interactions are responsible for rapid wave growth<sup>22,23,55,64,70</sup> and amplitude modulation of the waves.<sup>29,31</sup>

Basic theoretical approaches allowing the description of particle trapping by intense waves in the inhomogeneous plasma of the magnetosphere were first laid down in Refs. 28, 29, 50, and 51 (see also reviews of Refs. 6, 57, and 62). Next, modern spacecraft observations provided comprehensive statistical informations about the occurrence rate and other parameters of intense whistler and EMIC waves in the radiations belts,<sup>1,2,36,37,43,77</sup> stimulating further investigations of nonlinear wave-particle interactions.<sup>13,14,38,58,71,72</sup>

However, the important problem of the stability of the particles' trapped motion has often been left aside in previous works—except for a few studies devoted to the effects of wave amplitude modulations<sup>72,73</sup> or the simultaneous interactions of particles with several waves.<sup>24,52,65</sup> The latter

studies consider the presence of overlapping resonances from two (or more) waves in the system (see Refs. 65 and 87). One most remarkable case of this kind is the situation where sideband waves are present very close to the main wave.<sup>24,52</sup> Then, one deals with simultaneous resonant interaction with several waves, where particle trapping into one wave is destroyed by electromagnetic field perturbations induced by the other waves.

Besides this resonant destruction of trapping due to sidebands, however, one can also consider a mechanism of *non-resonant* destruction.<sup>17</sup> When trapped particles are transported by intense waves over quite long time intervals, they can be affected by various small-amplitude non-resonant fluctuations of the background electromagnetic field. Such additional fluctuations, while being generally too weak and too far from resonance to significantly perturb particle trajectories, may be used to control the fine regime of wave-particle resonant interaction and, thus, can eventually result in particle detrapping.<sup>82</sup> The cumulative effect of such electromagnetic field fluctuations can be estimated following an approach developed in Refs. 10 and 11. Below, we apply this kind of approach to a rather general system of trapped particle motion. The obtained results are used to estimate the stability of particle trapping by intense whistler-mode waves and EMIC waves in the Earth's radiation belts.

Of course, the considered non-resonant (diffusive) scattering of trapped particles is not as effective as a resonant perturbation: If trapped particles are influenced by a perturbation at the trapping frequency (in case of sideband

<sup>a)</sup>Also at Space Research Institute, RAS, Moscow, Russia. Electronic mail: ante0226@gmail.com

<sup>b)</sup>Also at National Taras Shevchenko University of Kiev, Kiev, Ukraine.

<sup>c)</sup>Also at Space Research Institute, RAS, Moscow, Russia.

instability<sup>24,52</sup>), then a resonance occurs and detrapping should be much more rapid than for a diffusive detrapping. Thus, the scenario examined in this paper actually corresponds to systems composed of one intense (chorus or EMIC) wave propagating in the midst of low amplitude non-resonant magnetic fluctuations separated in frequency from the main wave by a shift much larger than the trapping frequency. In such a scenario, sidebands as well as other waves susceptible of resonance overlap with the main wave are assumed to have negligible amplitudes (typically  $<0.1$  of the main wave amplitude).

## II. GENERAL EQUATIONS

In the strong magnetic field of the Earth's dipole  $\mathbf{B}(\mathbf{r})$ , the dynamics of charged particles (with velocity  $v$ , rest mass  $m$ , and charge  $e$ ) follows a hierarchy of three different quasi-periodic motions:<sup>60</sup> the fastest motion is the gyrorotation at the local gyrofrequency  $\Omega_c/\gamma$  (where  $\Omega_c = eB(\mathbf{r})/mc$  and  $\gamma = 1/\sqrt{1 - v^2/c^2}$  is the relativistic factor), the next one consists in bounce oscillations along field lines, and the slowest motion is an azimuthal rotation around the Earth. The resonant interaction of particles with whistler-mode and EMIC waves can significantly perturb the first two types of motions, while the timescale of resonant interaction is small enough to consider that the particle position in the azimuthal direction remains unchanged. Thus, we deal with a two-dimensional system describing particle motion along a geomagnetic field line (the corresponding coordinate is  $r_{\parallel}$ ) and across the field line (the corresponding coordinate is  $r_{\perp}$ ). Gyro-averaging transforms the coordinate  $r_{\perp}$  (and its conjugated momentum) to the first adiabatic invariant (i.e., the magnetic moment). Therefore, this system includes both particle bounce oscillations with a velocity  $\sim \dot{r}_{\parallel}$  and the eventual resonant interaction with waves. The wave phase is  $\phi = \text{const} + \int k_{\parallel}(r_{\parallel})dr_{\parallel} - \int \omega(t)dt + \Theta$ , where  $k_{\parallel}$  is the component of the wave vector parallel to the background magnetic field direction,  $\omega(t)$  is the wave frequency, and  $\Theta$  is the gyrophase with  $\dot{\Theta} = \Omega_c/\gamma$  (see, e.g., Ref. 60). The characteristic inhomogeneity scalelength along field lines is determined by the parameter  $R_0 = R_E L$ , with  $R_E$  the Earth's radius and  $L$  the so-called  $L$ -shell (we consider mainly the outer radiation belt with  $L \sim 5$ ). A rough estimate of the bounce frequency of relativistic electrons yields  $\sim c/R_0$ . The timescale of  $\phi$  variations is about  $\Omega_c$  ( $\dot{\phi} \sim k_{\parallel}\dot{r}_{\parallel} - \omega + \Omega_c/\gamma$ ). Thus, the wave phase varies with time much faster than particles move along field lines:  $\Omega_c R_0/c \gg 1$  (a similar relation can be obtained for the first term of  $\dot{\phi}$ :  $\chi = kR_0 \gg 1$ ).

The clear separation of the different timescales of particle motion determines the approach used to describe wave-particle resonant interactions. The Hamiltonian equations of charged particle dynamics are expanded around the resonance  $\dot{\phi} = 0$ , and one can consider particle motion in the  $(\phi, P)$  plane, where  $P$  is the momentum conjugate to  $\phi$ , for a frozen value of  $r_{\parallel}$ . For trapped particles, the system can be averaged over this periodic motion.<sup>3,4,63,67</sup> Such an averaged system describes the evolution of particle energy and

magnetic moment along the resonant trajectory  $r_{\parallel}(t)$ , where  $\dot{r}_{\parallel} = v_R$  is a solution of the equation  $\dot{\phi} = 0$

$$v_R = \frac{\omega(t) - n\Omega_c(r_{\parallel})}{\gamma k_{\parallel}(r_{\parallel})}. \quad (1)$$

The time  $t$  along a trajectory can be recalculated from the coordinate  $r_{\parallel}$  with the equation

$$t = \int^{r_{\parallel}} dr'_{\parallel} / v_R(r'_{\parallel}). \quad (2)$$

In Eq. (1),  $n=0$  corresponds to Landau resonance, while  $n=1$  corresponds to first cyclotron resonance. The combination of Eqs. (1) and (2) gives the implicit solution  $t = t(r_{\parallel})$  (although this solution often cannot be found analytically in realistic systems).

To investigate the possible destruction of the trapped motion, we should consider particle dynamics in the  $(\phi, P)$  plane.<sup>10,11</sup> For monochromatic waves, this dynamics is described by the following Hamiltonian equations:<sup>5,7,59</sup>

$$\begin{cases} \dot{P} = \Omega_{tr}^2(\sin \phi + A) \\ \dot{\phi} = gP, \end{cases} \quad (3)$$

where  $g(s)$ ,  $A(s)$ , and  $\Omega_{tr}^2(s)$  are functions of the coordinate along the resonance trajectory  $s = r_{\parallel}/R_0$  (and  $\dot{s} = v_R(s)/R_0$ ). The so-called trapping frequency  $\Omega_{tr}$  can be written as (for relativistic particles)

$$\Omega_{tr} = \sqrt{keB_w/mw(s)}, \quad (4)$$

where  $B_w$  is the wave magnetic field amplitude and  $w(s)$  is a dimensionless function of the order of 1. For very low energy particles with velocity  $\sim v_0 \ll c$ , there is an additional multiplicative factor  $\sqrt{v_0/c}$  in Eq. (4).

Equation (3) corresponds to the Hamiltonian

$$H = \frac{1}{2}gP^2 + \Omega_{tr}^2(\cos \phi - A\phi). \quad (5)$$

As  $\phi$  varies much faster than  $s$ , one can consider Eq. (5) as the Hamiltonian of a mathematical pendulum with torque and slowly varying parameters. In the case  $a < 1$ , the phase portrait of the Hamiltonian (5) contains closed trajectories (see Fig. 1(a)). Particles moving along these trajectories oscillate around  $P=0$  (i.e., around  $\dot{\phi} = 0$ ). Thus, for such particles, the resonance condition remains satisfied—such particles are trapped by the wave. The periodicity of trapped particle motion in the  $(\phi, P)$  plane allows to introduce the action  $I = (2\pi)^{-1} \oint Pd\phi$  (see Ref. 35). To briefly explain the meaning of the trapping frequency  $\Omega_{tr}$ , one can consider a particle trajectory oscillating around the bottom of the potential well in the  $(\phi, P)$  plane (see Fig. 1(b)). The coordinate  $\phi_0$  at the bottom corresponds to the extremum of the potential energy  $U = \Omega_{tr}^2(\cos \phi - A\phi)$ , yielding  $\sin \phi_0 = -A$ . Expanding the Hamiltonian (5) around  $\phi_0$  gives

$$H = \frac{1}{2}gP^2 + \frac{1}{2}\Omega_{tr}^2(\phi - \phi_0)^2 + \text{const}. \quad (6)$$

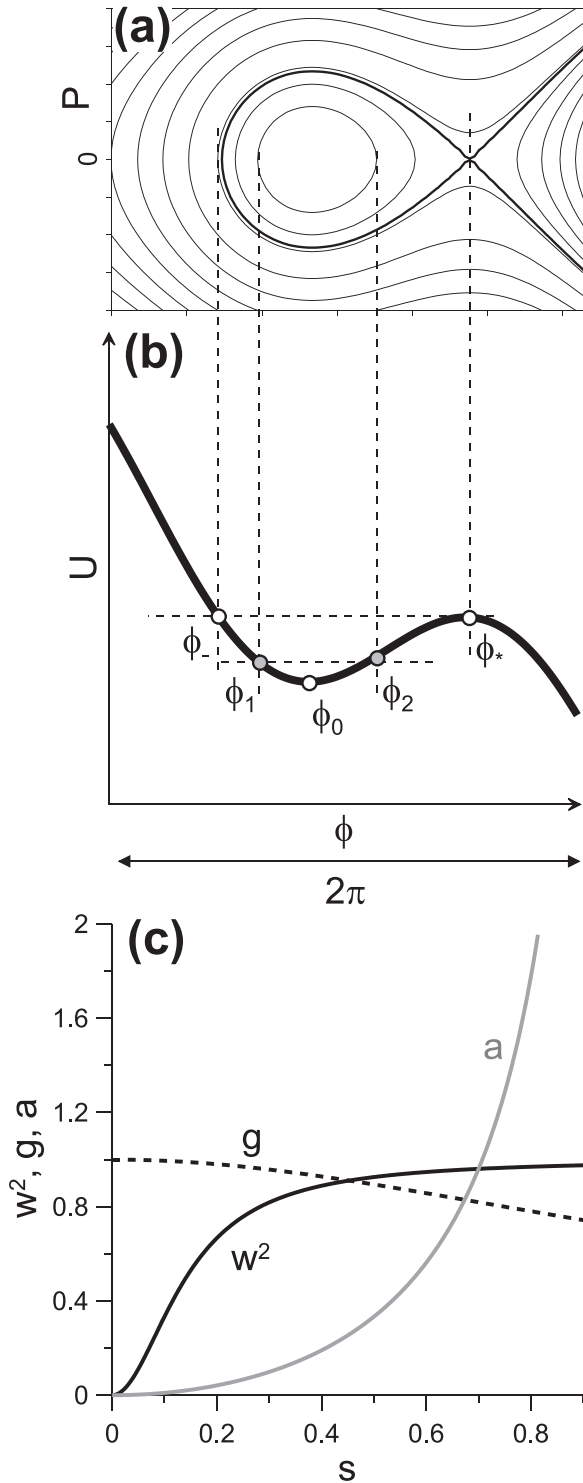


FIG. 1. (a) Phase portrait of the Hamiltonian (5) with  $a < 1$ ; (b) effective potential  $U = \Omega_{tr}^2 (\cos \phi - a\phi)$  of Hamiltonian (5) with  $a < 1$ ; and (c) profiles of model functions  $a(s)$ ,  $w^2(s)$ , and  $g(s)$ .

Equation (6) shows that  $g\Omega_{tr}$  is the frequency of particle oscillations in the  $(\phi - \phi_0, P)$  plane. The factor  $g = 1$  for nonrelativistic systems (for which the frequency  $\Omega_{tr}$  was initially introduced<sup>28–30,50,51</sup>), while for relativistic systems the factor  $g$  is responsible for a modification of the trapping frequency. Although  $g\Omega_{tr}$  represents the frequency of trapped particle oscillations only in the vicinity of the bottom of the potential well, this term can be used to estimate the

frequency of oscillations of trapped particles over almost the entire region filled by closed trajectories (except near its boundary), because the actual frequency of trapped particle oscillations depends very weakly on  $I$ —i.e., on the position of a particle within this region (see, e.g., Refs. 4 and 80). It allows us to use hereafter  $2\pi/(g\Omega_{tr})$  as an estimate of the period of trapped particle oscillations. This period is small as compared with the typical timescale of  $s$  variations, because  $\Omega_{tr}^2 \sim kc\dot{s}$  and  $kc \gg \dot{s}$ .

In a system with constant  $s$ , the particle trajectory in the  $(\phi, P)$  plane does not evolve and, thus, the area surrounded by this particle trajectory is exactly conserved. In the more realistic case of a slow enough variation of  $s$  (when the time scale of the  $s$  variations is much larger than the period  $\sim 2\pi/\Omega_{tr}$ ), the action  $I$  becomes an adiabatic invariant of the system,<sup>8,35</sup> i.e., the area  $2\pi I$  is still conserved to a high degree of accuracy even if the effective potential  $U$  varies with  $s$  (with time). Thus,  $I$  can be used to characterize the trapped particle motion.

Generally, in the saturated stage of wave instability away from the equator, the function  $a(s) = \Omega_{tr}^2 A(s)$  does not depend anymore on wave amplitude, being mostly determined by the gradients of the system. For each particular system,  $a(s)$  can be found using the expansion of the initial equations of motion around the resonance  $\phi = 0$ . In the particular case of the gyroresonant (i.e., first cyclotron resonance) interaction of relativistic electrons with whistler-mode waves, the expression for  $a$  contains three terms:<sup>20,21,54,56</sup>  $\sim \partial\omega/\partial t$ ,  $\sim (kc^2/\Omega_c)\partial\Omega_c/\partial s$ , and  $\sim v_R\partial\Omega_c/\partial s$ . In case of a significant gradient in  $k_{\parallel}(s)$ , one would get an additional (fourth) term  $\sim v_R^2\partial k_{\parallel}/\partial s$  (see, e.g., Refs. 9 and 62). For EMIC waves, the function  $a$  can be found in Refs. 5 and 59. It is also worth noting that the function  $a \sim \Omega_{tr}^2$  during strong wave-particle interaction such as trapping and nonlinear scattering,<sup>9,56</sup> corresponding to a normalized wave amplitude of the same order of magnitude as the gradients of the system parameters:  $B_w/B \sim v_R/(\Omega_c R_0)$ .

Since we aim at investigating the potential disruption of trapped particle motion by additional magnetic fluctuations in the most general case, we consider below a very generic system corresponding to electron trapping by an intense wave. Such a standard wave-particle system can easily be used for various applications. Although the considered system does not correspond to any particular wave mode, we do use model profiles  $g(s)$ ,  $a(s)$ , and  $w^2(s)$  similar to realistic profiles discussed in Refs. 3, 9, and 62. Namely, we take  $g(s) = 1/\sqrt{1+s^2}$  (for nonrelativistic systems there is a multiplication factor  $(v_0/c)^2$  before  $s^2$ ),  $a(s) = s^2(1-s^2)^{-1}$ ,  $w^2 = s^2/(s_0^2 + s^2)$ , where  $s_0 = 0.15$  is a typical scale length of increase of wave intensity in the Earth's radiation belts around  $L \sim 5$  (see Refs. 1, 9, and 44). The fact that  $a = 0$  at the equatorial plane  $s = 0$  means that we do not take into account the term  $\sim \partial\omega/\partial t$  (only this term has a finite value at  $s = 0$  because the magnetic field gradient  $\partial\Omega_c/\partial s$  and wave number gradient  $\partial k_{\parallel}/\partial s$  both vanish at  $s = 0$  due to the symmetry of the geomagnetic field model and wave propagation, see details in Refs. 20, 21, 54, and 56). The profiles of coefficients  $a(s)$ ,  $w^2(s)$ , and  $g(s)$  are presented in Fig. 1(c).

Let us first examine the trapped motion of particles in the presence of an intense wave and demonstrate the conservation of  $I$ . We introduce the dimensionless wave amplitude  $\varepsilon = kR_0 B_w / B_0$  and renormalize time as  $t \rightarrow t\omega_*$  with  $\omega_* = \sqrt{\Omega_{c0} c / R_0}$ . In this case, the Hamiltonian (5) takes the form

$$H = \frac{1}{2}gP^2 + \varepsilon w^2 \cos \phi - a\phi. \quad (7)$$

Trapped trajectories exist in the region where  $\varepsilon w^2(s) > a(s)$ . Consider the solution of Hamiltonian equations  $\dot{\phi} = \partial H / \partial P$ ,  $\dot{P} = -\partial H / \partial \phi$  for a particle trajectory initially trapped at  $s = s_0$ . We slowly vary  $s > s_0$  and study the particle motion in the  $(\phi, P)$  plane. Figure 2 shows the particle trajectory and the action  $I$ :

$$I = \frac{1}{2\pi} \oint P d\phi = \frac{1}{\pi} \sqrt{\frac{2}{g}} \int_{\phi_1}^{\phi_2} \sqrt{H - \varepsilon w^2 \cos \phi + a\phi} d\phi, \quad (8)$$

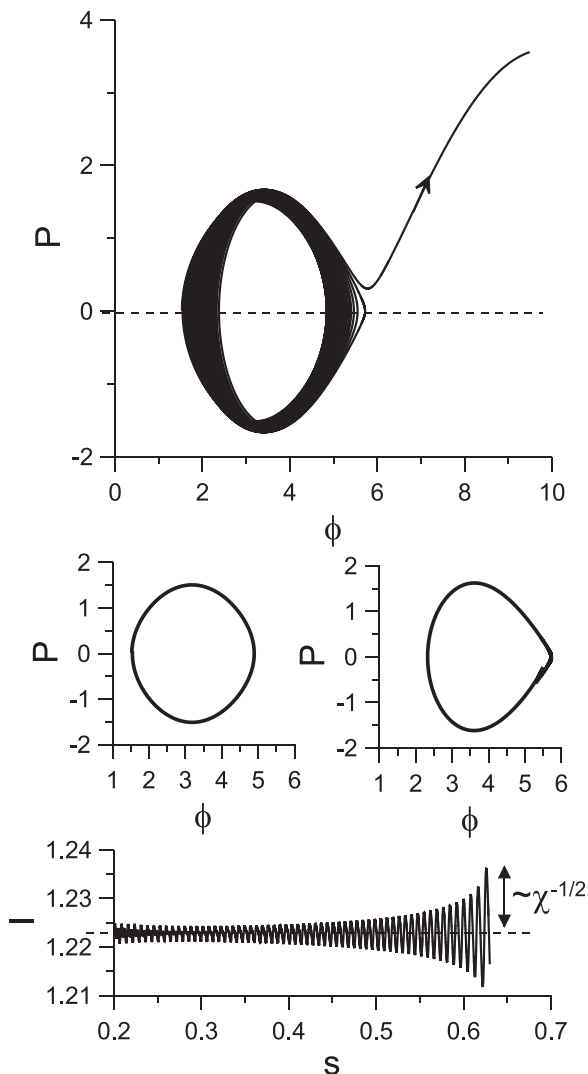


FIG. 2. A test particle trajectory in the  $(\phi, P)$  plane and the corresponding  $I$  profile (shown only for  $s$  values corresponding to the trapped motion). The middle panel shows two fragments of the trajectory in the  $(\phi, P)$  plane (at the beginning and just before the escape from resonance).

where  $\phi_{1,2}$  are shown in Fig. 1(b). The variations of parameters  $g$ ,  $w$ , and  $a$  result in the observed evolution of the particle trajectory in the  $(\phi, P)$  plane, but the action  $I$  is conserved. There are only very small amplitude  $\sim \chi^{-1/2}$  ( $\chi = kR_0 \gg 1$ ) oscillations of  $I$ , corresponding to the fact that integral (8) is calculated for a frozen  $s$ , while there are actually small variations of  $s$  within one period of trapped particle oscillations in the  $(\phi, P)$  plane.

Let us consider a whole cycle of charged particle motion, including particle trapping and escape from resonance. To this aim, we start the numerical integration at  $s = 0$ , choose a large enough  $\varepsilon$ , and select a trajectory which is trapped (see Fig. 3). The conservation of  $I$  for trapped particles means that we can use it to determine the moments of time when a particle enters and escapes from the resonance. At the start of trapping, the value of  $2\pi I$  is equal to the area surrounded by the boundary of the region filled by closed trajectories in the  $(\phi, P)$  plane. This boundary is called the separatrix, and the corresponding area  $S$  is defined as (see, e.g., Refs. 8, 12, 27, and 48)

$$S = 2\sqrt{\frac{2a}{g}} \int_{\phi_-}^{\phi_*} \sqrt{\frac{\varepsilon w^2}{a} (\cos \phi_* - \cos \phi) - \phi_* + \phi} d\phi, \quad (9)$$

where  $\phi_- = \phi_-(s)$  is a solution of the equation  $\varepsilon w^2(s) \sin \phi = -a(s)$  different from  $\phi_*$  (both  $\phi_*$  and  $\phi_-$  are shown in Figs. 1(a) and 1(b)). The area  $S(s)$  varies with  $s$ , while  $I$  is conserved. Thus, the trapped particles escape from the resonance when  $S$  becomes equal to  $2\pi I$  while  $dS/ds < 0$  (i.e., when the area surrounded by the separatrix becomes smaller than the area surrounded by the trapped particle trajectory so that the particle escapes into the region with open trajectories). An example of particle escape from the resonance is shown in Fig. 3: it occurs exactly when  $S$  becomes equal to  $2\pi I$  (or to the value of  $S$  at the start of trapping).

Figures 2 and 3 demonstrate that the trapped motion is the result of the conservation of the adiabatic invariant  $I$  in the main wave-particle system. However, if an additional (external) force inducing variations of  $I$  were to be present too, then  $2\pi I$  could become equal to  $S$ , leading to a corresponding escape of the particle from resonance. In Section III, we consider the effects of such an external force and demonstrate that it may eventually lead to the destruction of the adiabatic invariant  $I$ .

### III. MAGNETIC FIELD FLUCTUATIONS

In this section, we consider the effect of additional magnetic field fluctuations on trapped particle motion. For the sake of generality, these fluctuations are assumed to be mostly non-resonant, i.e., their frequency, although being of the same order as the main wave frequency, is assumed to differ sufficiently from it to allow neglecting resonant interactions between particles trapped by the main wave and these fluctuations (in contrast to cases considered in Refs. 52 and 65). Moreover, we consider here fluctuations parallel to the geomagnetic field line (transverse fluctuations will be briefly addressed in Section V; see also Ref. 17). It may

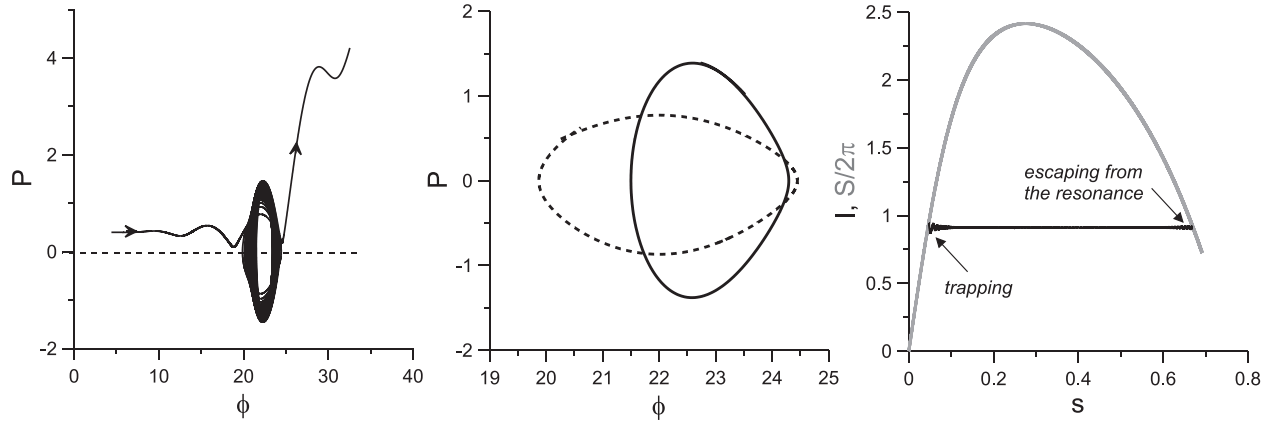


FIG. 3. A test particle trajectory in the  $(\phi, P)$  plane. The middle panel shows two fragments of the trajectory in the  $(\phi, P)$  plane: just after trapping (dashed curve) and just before the escape (solid curve).  $I$  and  $S$  profiles are shown in the right panel.

correspond to whistler-mode fluctuations with wave-normal angle  $\theta \sim 30^\circ - 60^\circ$  (their parallel magnetic component being then of the same order as their perpendicular components). Such fluctuations can be included into the term  $\sim a$  in Hamiltonian (5). There are two terms corresponding to magnetic field fluctuations: The first term comes from the dependence of  $a$  on  $B$ , and the second term comes from the dependence of  $a$  on the derivative  $\partial B/\partial s$ . As we assume that magnetic field fluctuations are fast and small-scale, the second term dominates. Thus, we can write  $a = a_0 + (a_0/\partial B/\partial s)\partial\delta B/\partial s$ , where  $a_0$  depends only on the non-fluctuating background magnetic field  $B$ , while  $\delta B(s, t)$  denotes magnetic field fluctuations.

In this paper, we consider hereafter a very simplified model of coherent quasi-stationary magnetic field fluctuations with a typical spatial scale  $\ell R_0$ . For particles moving at the velocity  $v_R$  in the resonance with the main (intense) wave, such fluctuations appear as spatio-temporal fluctuations with a timescale  $\tau \sim \ell R_0/v_R$ . Thus, one can write  $\partial\delta B/\partial s \sim \delta B/\ell$ . This prototypical model of fluctuations can be considered as a very rough representation of a noise-like distribution of quasi-standing fluctuations composed of a mixture of counter-propagating waves with a typical overall scale length  $\ell R_0 \sim \lambda$ —the wide spectrum of  $\lambda$  values usually associated with incoherent fluctuations is ignored for the sake of both simplicity and generality. The above generic model of fluctuations can also be adopted to describe coherent fluctuations corresponding to additional low-amplitude whistler-mode waves with frequency  $\omega_f$  and wavenumber  $k_f$ . In the latter case, one can simply replace  $|v_R|$  by  $|v_{eff}| = |v_R - \omega_f/k_f|$  giving the relative velocity of such fluctuations in the frame of moving electrons. We discuss these different applications further below.

As we do not specify the type of function  $a$ , we can assume that  $(a_0/\partial B/\partial s)\partial\delta B/\partial s \approx a_1(\delta B/B_0)R_0/\tau v_{R0}$  while all numerical factors (of order unity) and the dependence on  $s$  are included into the  $a_1(s)$  function ( $v_{R0}$  is the equatorial resonant velocity, and  $B_0$  the equatorial geomagnetic field amplitude). In this case, the Hamiltonian (5) takes the form

$$H = \frac{1}{2}gP^2 + \omega_*^2(\varepsilon w^2 \cos \phi - a_0\phi) - \omega_{**}^2 a_1 \delta b \phi, \quad (10)$$

where  $\omega_* = \sqrt{\Omega_{c0}c/R_0}$ ,  $\omega_{**} = \sqrt{\Omega_{c0}c/v_{R0}\tau}$ , and  $\delta b = \delta B/B_0$ . To keep a general approach, we do not specify the type of fluctuations  $\delta B$  but simply introduce two parameters characterizing these fluctuations: their timescale  $\tau$  and variance  $\text{Var}(\delta B) = \sigma$  (the corresponding spectral power of fluctuations is  $\sigma\tau$  in  $\text{pT}^2/\text{Hz}$ ). Magnetic field fluctuations are assumed to be high-frequency, such that  $\tau\Omega_{tr} \ll 1$ , and both fast variables  $(\phi, P)$  and slow variable  $s$  change only weakly over one time step (time interval  $\sim\tau$ ) of fluctuations.

Following the scheme proposed in Ref. 10, we calculate the jump of the adiabatic invariant of trapped particles  $\Delta I$  over one time step ( $\sim\tau$ ) of fluctuations. According to the definition  $\Omega_{tr}g = \partial H/\partial I$  (see Ref. 35), we have

$$\Delta I = \frac{1}{\Omega_{tr}g} \Delta H = -\frac{1}{\Omega_{tr}g} \omega_{**}^2 a_1 \delta b \Delta \phi, \quad (11)$$

where all functions on the right-hand side of Eq. (11) are evaluated at the same moment within one time step of fluctuations, while  $\Delta\phi$  is the change of  $\phi$  between the beginning and end of this step. This change  $\Delta\phi$  can be obtained after integration of the Hamiltonian equation  $\dot{\phi} = \partial H/\partial P = gP$  over a small time step  $\tau$ :  $\Delta\phi = gP\tau$ , while both  $g$  and  $P$  are evaluated at the same moment within one step. Thus, Eq. (11) can be rewritten as

$$\Delta I = -\frac{1}{\Omega_{tr}} \omega_{**}^2 a_1 \delta b P \tau. \quad (12)$$

On the right-hand side of Eq. (12),  $\delta b$  changes much faster than  $P$ , and both functions  $\delta b$  and  $P$  are changing faster than functions  $g(s)$ ,  $\Omega_{tr}(s)$ ,  $a_1(s)$ . Thus, we can consider a time interval including many steps  $\sim\tau$ , but short enough to keep  $s$  unchanged. We can choose this interval equal to  $2\pi/g\Omega_{tr}$  corresponding to one period of particle oscillations in the  $(\phi, P)$  plane. Over this time interval, the variance of  $\Delta I$  is

$$\text{Var}(\Delta I) = \left( \frac{\omega_{**}^2 a_1 \tau}{\Omega_{tr}} \right)^2 \text{Var}(\delta b P). \quad (13)$$

We assume that fluctuations  $\delta b$  and variations of  $P$  are statistically independent and, thus,  $\text{Var}(\delta b P) = (\sigma/B_0^2) \text{Var}(P)$ . The term  $\text{Var}(P)$  can be considered as a sum of  $M \gg 1$  values of

$P^2$  calculated within consecutive time steps  $\tau$  (i.e., between successive changes of  $\delta b$ )

$$\begin{aligned} \text{Var}(P) &= \frac{1}{M} \sum_{i=0}^M P_i^2 = \frac{\sum_i P_i^2 \tau}{\sum_i \tau} \\ &\approx \frac{g\Omega_{tr}}{2\pi} \oint P^2 dt = \frac{\Omega_{tr}}{2\pi} \oint P d\phi = \Omega_{tr} I, \end{aligned} \quad (14)$$

where we took into account the smallness of the time step  $\tau$ . Substituting Eq. (14) into Eq. (13), we obtain

$$\text{Var}(\Delta I) = \frac{\omega_{**}^4 a_1^2}{\Omega_{tr} B_0^2} I \sigma \tau^2. \quad (15)$$

The evolution of  $I$  can be viewed as a random walk and described by the diffusion equation for the distribution  $\Psi(I)$  of trapped particles as a function of  $I$

$$\frac{\partial \Psi}{\partial t} = \frac{\partial}{\partial I} \left( D_{II} \frac{\partial \Psi}{\partial I} \right). \quad (16)$$

In Eq. (16), we introduced the diffusion coefficient  $D_{II} = \text{Var}(\Delta I)/\tau$ . Performing a change of coordinate from  $t$  to  $s$  (via  $\dot{s} = v_R/R_0$ ) in Eq. (16) and introducing  $u_R = v_R/v_{R0}$ , with  $v_{R0}$  the resonant velocity at the equator, we get

$$\frac{\partial \Psi}{\partial h} = \frac{\partial}{\partial I} \left( I \frac{\partial \Psi}{\partial I} \right), \quad (17)$$

where

$$h = \frac{\omega_{**}^4 R_0 \sigma \tau}{\Omega_{tr} v_{R0} B_0^2} \int \frac{w(s) a_1^2(s') ds'}{w(s') u_R(s')}. \quad (18)$$

The boundary of the region filled by trapped trajectories is determined by the value of the area  $S$  surrounded by the separatrix (see Eq. (9)). Again omitting all numerical factors of order unity, we get  $S \approx \Omega_{tr}$  (we assume that  $\varepsilon \omega^2 > a$  and, thus, in dimensional form  $S \sim \omega_* \sqrt{\varepsilon} W \sim \Omega_{tr}$ ). Renormalizing  $i = 2\pi I/S$ , we can rewrite Eq. (17) in dimensionless form

$$\frac{\partial \Psi}{\partial K} = \frac{\partial}{\partial i} \left( i \frac{\partial \Psi}{\partial i} \right), \quad (19)$$

where

$$\begin{aligned} K &= \frac{2\pi \omega_{**}^4 R_0 \sigma \tau}{\omega_*^2 \varepsilon v_{R0} B_0^2} \int \frac{a_1^2(s') ds'}{w(s') u_R(s')} \\ &= \frac{2\pi}{\omega \tau B_w B_0 \Omega_{c0}} \left( \frac{c}{v_{R0}} \right)^2 k R_0 F_1(s) = K_0 F_1(s). \end{aligned} \quad (20)$$

Equation (19) describes the temporal evolution of the distribution  $\Psi(i)$  of trapped particles. Thus, for a given initial distribution, one can easily calculate the number of particles remaining trapped for a given value of  $K$ . Solutions of Eq. (19) are shown in Fig. 4 for three types of initial distributions: (a) A uniformly filled region of trapped particles, (b) trapped particles present only at the bottom of the potential well, and (c) only recently trapped particles with  $i \sim 1$  are present. The right panel of Fig. 4 shows that in all three cases, the number of trapped particles diminishes as  $K$  increases, ultimately decreasing to 50%–20% already for  $K=0.2$ . Consequently, to estimate the amount of detrapped (escaped) particles in realistic systems, one simply needs to evaluate  $K = K_0 F_1(s)$ , where  $F_1(s)$  is of order unity. As trapped motion corresponds to  $s \in [0, 1]$ , the dependence of  $K$  on  $s$  can be further neglected, considering it merely as a multiplicative factor  $\sim 1$ . In the end, the occurrence of a significant detrapping of electrons is simply equivalent to the condition  $K_0 = 0.2$ , where  $K_0$  is a function of the wave amplitude, the intensity of magnetic field fluctuations, and other wave parameters. Solving this equation  $K_0 = 0.2$  for different realistic systems, we can deduce the intensity of magnetic field fluctuations required to detrapp a significant population of particles.

### A. Turning acceleration by whistler waves

In this subsection, we consider particle trapping in the first cyclotron resonance with parallel propagating whistler-mode waves (one of the most classical examples of electron acceleration in the radiation belts, see, e.g., Refs. 15, 28, 29, 50, and 51 and reviews Refs. 62 and 76). In this regime of particle acceleration, the resonant velocity  $v_R$  is

$$v_R = (\omega \gamma - \Omega_c) / k \gamma. \quad (21)$$

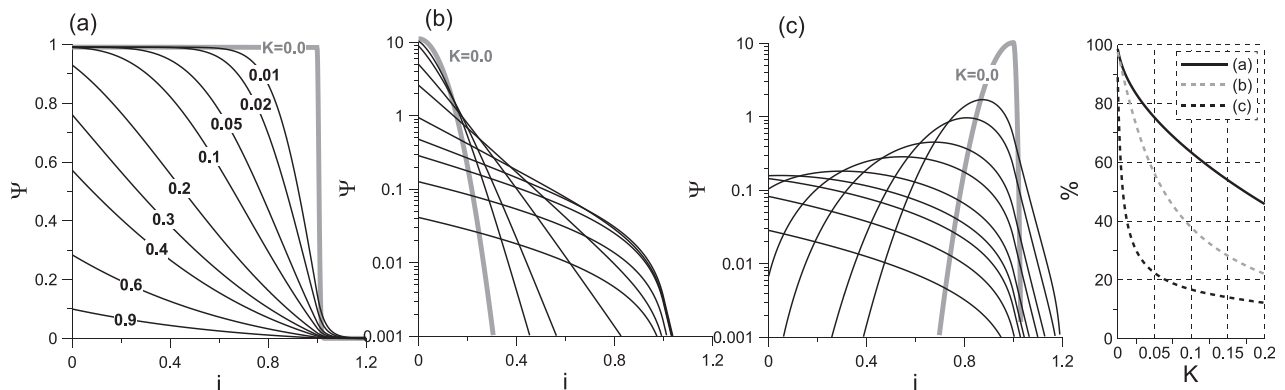


FIG. 4. Three examples of evolution of distributions of trapped particles  $\Psi(i)$ . All particles with  $i > 1$  are assumed to escape from the system within a very short time interval. The right panel shows the evolution of the number of trapped particles for these three examples.

For particles with energy  $\gamma < \Omega_c/\omega$  (i.e., for energies lower than  $\sim 1$  MeV),  $v_R$  is negative and trapped particles propagate in the direction opposite to the wave. However, if in the course of trapped particle acceleration, the energy increases enough to get  $\gamma > \Omega_c/\omega$ , then the trapped particle's direction of propagation is reversed (the so-called turning acceleration, see Refs. 25, 54, and 69). The total duration of trapped motion is rather long, leaving some room for the occurrence of a diffusive destruction of the trapping process.

As a first step, one can simply take  $\gamma \sim 1$  and thus  $|v_{R0}| = \Omega_{c0}(1 - \omega/\Omega_{c0})/k$  to estimate the disturbance to the trapping process of 50 – 150 keV electrons induced by additional magnetic field fluctuations. Equation (20) can then be rewritten as

$$K_0 = \frac{2\pi \sigma N^3 \Omega_{c0} R_0}{\omega \tau B_w B_0 c} \frac{(\omega/\Omega_{c0})^4}{(1 - \omega/\Omega_{c0})^2}, \quad (22)$$

where  $N = kc/\omega$  is the wave refractive index

$$N^2 = \frac{k^2 c^2}{\omega^2} = \frac{\omega_{pe}^2}{\Omega_c^2} \frac{\Omega_c/\omega}{(1 - \omega/\Omega_c)}, \quad (23)$$

where  $\omega_{pe}$  is the plasma frequency. Evaluating  $N$  at the equatorial plane, we rewrite Eq. (22) as

$$K_0 = \frac{2\pi \sigma \omega_{pe}^3 \Omega_{c0} R_0}{\omega \tau B_w B_0 \Omega_{c0}^3 c} \frac{(\omega/\Omega_{c0})^{5/2}}{(1 - \omega/\Omega_{c0})^{7/2}}. \quad (24)$$

We use the empirical plasmatrough density model from Ref. 61 to estimate the ratio  $\omega_{pe}/\Omega_{c0} \sim L$  as a function of  $L$ -shell. In the Earth's magnetosphere, the ratio  $R_0 \Omega_{c0}/c$  is about  $\sim 1.1 \times 10^3 L^{-2}$  for  $B_0 \approx 3.06 \times 10^4 \text{ nT}/L^3$ . Thus, Eq. (24) finally takes the form

$$K_0 \approx 2.3 \times 10^{-3} \cdot \frac{2\pi}{\omega \tau} \left( \frac{\sigma/\text{pT}^2}{B_w/\text{nT}} \right) \left( \frac{L}{5} \right)^4 \frac{(\omega/\Omega_{c0})^{5/2}}{(1 - \omega/\Omega_{c0})^{7/2}}. \quad (25)$$

We consider quasi-stationary magnetic field fluctuations with an effective frequency  $2\pi/\tau$  comparable to the frequency  $\omega$  of intense whistler-mode chorus waves responsible for particle trapping. Thus, one has  $2\pi/\omega\tau \sim 1$ . This generic model of fluctuations can be regarded as a very rough representation of a peaked noise spectrum. We plot in Fig. 5 (left panel) the power of magnetic fluctuations  $\sigma$  required to reach two values of  $K_0$  for  $L=5$  and various values of  $\omega/\Omega_{c0}$  and wave amplitude  $B_w$ . For a smaller wave frequency, stronger magnetic field fluctuations are necessary to significantly detrap the population of particles (i.e., to get  $K_0 = 0.2$ ). A realistic<sup>1,44</sup> average level of fluctuations  $\sigma^{1/2} \sim 6 - 20$  pT can markedly disrupt the trapping process even for rather high amplitudes  $B_w \sim 0.3 - 1$  nT of the main wave. For higher frequency waves (e.g., upper-band chorus waves with  $\omega/\Omega_{c0} > 0.5$ ), relatively weak fluctuations with  $\sigma^{1/2} \leq 10$  pT are sufficient to totally destroy the trapped motion (since  $K_0$  reaches one). Finally, for higher energy ( $\sim 0.3 - 1$  MeV) electrons, the  $\gamma$  factors must be retained, leading to an overall increase of  $K_0$  by a factor  $\sim \gamma(\Omega_{c0} - \omega)/|\Omega_{c0} - \gamma\omega| > 1$ . In the alternative case of really coherent whistler-mode fluctuations with  $k_f \sim k$ ,  $|v_{R0}|$  should be replaced by  $|v_{eff}| = |v_{R0} - \omega_f/k_f|$ . It corresponds to an extra multiplicative factor  $\sim |1 - \gamma\omega/\Omega_{c0}|$ , yielding ultimately similar  $K_0$  values as in Fig. 5 (left panel).

To demonstrate the effect of  $I$  invariant destruction, we have numerically integrated the Hamiltonian equations for Hamiltonian (10). With time normalized by  $\omega_*$ , this Hamiltonian takes the form

$$H = \frac{1}{2} g P^2 + \varepsilon w^2 \cos \phi - a_0 \phi - a_1 \delta \tilde{b} \phi, \quad (26)$$

where  $\delta \tilde{b}$  is given by the equation

$$\delta \tilde{b} \approx \frac{1}{60} \cdot \frac{2\pi}{\omega \tau} \left( \frac{\omega/\Omega_{c0}}{1 - \omega/\Omega_{c0}} \right)^{3/2} \left( \frac{L}{5} \right)^2 \sqrt{\frac{\sigma}{\text{pT}^2}} f(t), \quad (27)$$

where  $f(t)$  is a random function with a time-step of variation equal to  $\tau$  and an amplitude equal to one. We assume that  $f$

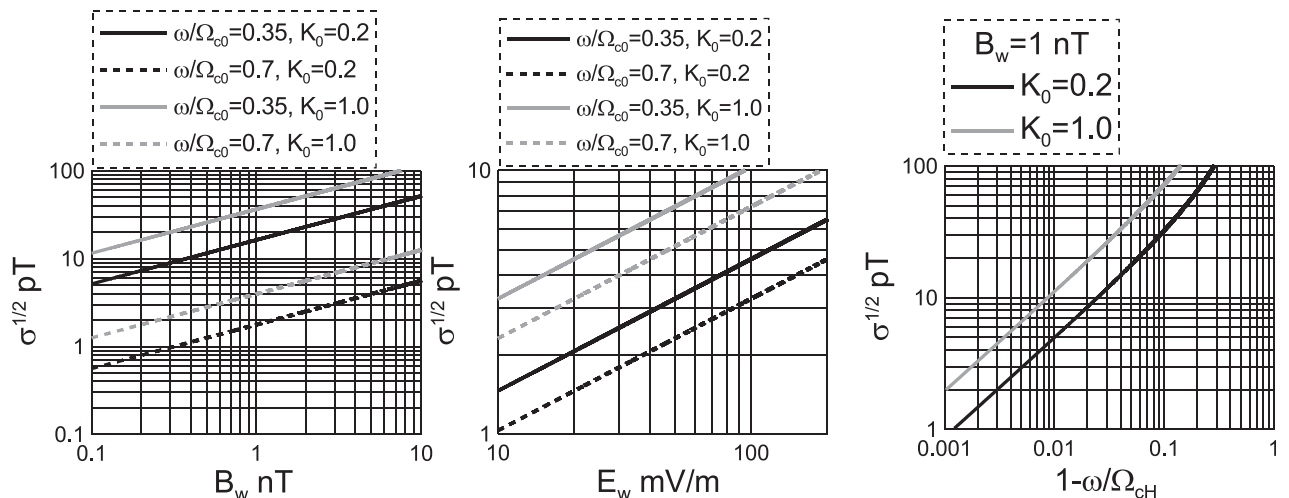


FIG. 5. Left and central panels: fluctuation amplitude  $\sqrt{\sigma}$  that corresponds to two values of  $K_0$  as a function of main parallel (left panel) and oblique (central panel) wave amplitude for two typical whistler-mode chorus wave frequencies  $\omega/\Omega_{c0}$ . Right panel shows amplitude  $\sqrt{\sigma}$  of magnetic field fluctuations corresponding to high frequency hiss-like waves with  $2\pi/\tau = 200\Omega_{cH}$  as a function of EMIC wave frequency  $\omega$  for different values of  $K_0$ .

has a uniform distribution within the interval  $[-1, 1]$ . For  $L \sim 5$ ,  $\omega/\Omega_{c0} \sim 0.5$ , and  $\tau \approx 2\pi/\omega$  we have  $\delta\tilde{b} \approx \sqrt{\sigma/pT^2 f(t)/60}$ . Figure 6 shows several examples of particle trajectories for  $a_1(s) = 1/(1-s^2)$  and different values of  $\sigma$ . Initially, all particles are located close to the bottom of the potential well ( $I_0$ , the initial value of  $I$ , is significantly smaller than  $S/2\pi$ ). In the absence of additional fluctuations ( $\sigma = 0$ ), the adiabatic invariant  $I$  is conserved and the particle escapes from the resonance when  $S = 2\pi I_0$ . In a system with magnetic field fluctuations ( $\sigma \neq 0$ ), however, the conservation of  $I$  is broken and the invariant may increase or decrease with time (the profile  $I(s)$  depends on realizations of the random function  $f$  along the trace). However, decreasing  $I$  does not change the type of motion (a particle remains trapped), but increasing  $I$  may cause detrapping. For that purpose, in Fig. 6, we chose trajectories with increasing  $I$ . A stronger fluctuation level corresponds to a larger rate of  $I$  variation and, as a result, to earlier particle escape from resonance

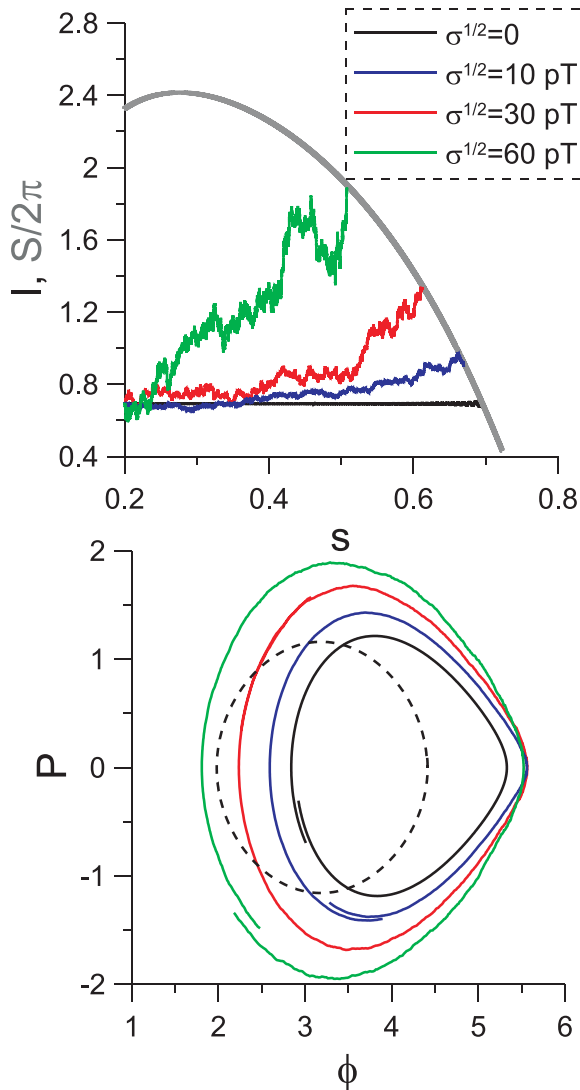


FIG. 6. The top panel shows the profile of the area  $S$  surrounded by the separatrix and several profiles of adiabatic invariants  $I$  calculated for different values of  $\sigma$ . The bottom panel shows fragments of particle trajectories in the  $(\phi, P)$  plane (the last period before escaping from resonance). The dashed curve in the bottom panel shows a fragment of particle trajectory at the initial time (it is the same for all trajectories).

when  $I = S/2\pi$ . The bottom panel of Fig. 6 shows the effective increase of the area surrounded by the particle trajectory in the  $(\phi, P)$  plane.

## B. Landau resonance with oblique whistler waves

Recent spacecraft observations have revealed the existence of a substantial population of very intense oblique whistler-mode waves in the radiation belts.<sup>2,18,19,84</sup> These waves propagate with a large angle  $\theta > \theta_g$  between their  $\mathbf{k}$ -vector and the background magnetic field (where  $\cos \theta_g = 2\omega/\Omega_{c0}$  and  $\theta_g$  is the so-called Gendrin angle<sup>26</sup>). Propagating in an almost electrostatic mode and having a large parallel electric field,<sup>2</sup> such oblique waves are able to trap energetic ( $\sim 10 - 100$  keV) electrons via the Landau resonance.<sup>9,53</sup> The corresponding frequency of trapped motion  $\Omega_{tr}$  is determined by the electric field amplitude  $E_w$ :  $\Omega_{tr} \approx \sqrt{keE_w/mw(s)}$ . The corresponding resonant velocity is  $v_{R0} = \omega/k_{\parallel} = \omega/(k \cos \theta)$ . Accordingly, we consider  $\theta = \theta_g$  and rewrite Eq. (20) for  $K_0$

$$K_0 = \frac{2\pi}{\omega\tau} \frac{4\sigma}{E_w B_0} N^3 \frac{\omega^4 \Omega_{c0} R_0}{\Omega_{c0}^4 c}. \quad (28)$$

The refractive index  $N$  for the Gendrin mode is  $N = kc/\omega = \omega_{pe}/\omega$ . Thus, substituting the numerical factors listed below Eq. (24) into Eq. (28), we readily obtain

$$K_0 \approx \frac{2\pi}{\omega\tau} \frac{\sigma/pT^2}{E_w/2.7 \text{ mV/m}} \left(\frac{L}{5}\right)^4 \frac{\omega}{\Omega_{c0}}. \quad (29)$$

Typical amplitudes of intense oblique chorus wave are within the range  $E_w \in [10, 200]$  mV/m (see, e.g., Refs. 2, 18, and 74). For  $\tau \sim 2\pi/\omega$  and given values of  $K_0$ , we plot in Fig. 5 (central panel) the corresponding fluctuation amplitude  $\sigma^{1/2}$  as a function of main wave amplitude  $E_w$ . At  $L \sim 5$ , where a substantial population of oblique chorus waves has been observed,<sup>1</sup> a moderate level of additional magnetic field fluctuations  $\sqrt{\sigma} \in [1, 10]$  pT appears to be sufficient to significantly destroy the trapped particle motion (at larger  $L$ -shells, the required level of  $\sigma$  is even smaller). If one considers coherent magnetic fluctuations corresponding to parallel whistler-mode waves with  $\omega_f \sim \omega$  and  $k_f \sim k$ ,  $|v_{R0}|$  must be replaced by  $|v_{eff}| = |v_{R0} - \omega/k|$  in  $K_0$ . It yields an additional multiplicative factor  $\sim 1/(1 - \cos \theta_g) > 1$  in  $K_0$  and therefore a slightly stronger effect.

## C. Cyclotron resonance with EMIC waves

Strong EMIC waves are observed by spacecrafts mainly during geomagnetically disturbed conditions and inside regions of enhanced plasma density on the duskside.<sup>43,81</sup> These waves play an important role in the scattering of relativistic and especially ultra-relativistic electrons and can ultimately precipitate them into the atmosphere.<sup>33,39,68,75</sup> Moreover, the very high intensity of EMIC waves leads to nonlinear wave-particle interactions, including the trapping of relativistic electrons.<sup>5,38,58,59</sup> Let us consider here the hydrogen band of EMIC waves.<sup>43,68</sup> The dispersion relation of such parallel EMIC waves is

$$N = \frac{ck}{\omega} = \sqrt{\frac{\omega_{pH}^2}{\Omega_{cH}(\Omega_{cH} - \omega)}}, \quad (30)$$

where the hydrogen plasma frequency is  $\omega_{pH} = \eta^{1/2}\omega_{pe}$ , and the proton gyrofrequency is  $\Omega_{cH} = \eta\Omega_{c0}$ , with  $\eta = m_e/m_H$  the electron to proton mass ratio. Since one has  $\omega \ll \Omega_{c0}$ , the corresponding electron velocity at cyclotron resonance is simply  $v_{R0} \approx \Omega_{c0}/(\gamma k)$  (e.g., see Ref. 68), while  $\gamma$  can reach 10–15 and must therefore be retained. Using Eq. (30), we rewrite Eq. (20) as

$$K_0 = \frac{2\pi \sigma \gamma^2 \eta^{5/2} \omega_{pe}^3}{\omega \tau B_w B_0} \frac{(\omega/\Omega_{cH})^4}{\Omega_{c0}^3 (1 - \omega/\Omega_{cH})^{3/2}} \frac{\Omega_{c0} R_0}{c}. \quad (31)$$

We substitute numerical estimates listed below Eq. (24) into Eq. (31)

$$K_0 \approx \frac{2\pi \gamma^2 (\omega_{pe}/\Omega_{c0})^3}{\omega \tau} \frac{\sigma/nT^2}{8 \cdot 10^6} \left(\frac{L}{5}\right) \frac{(\omega/\Omega_{cH})^4}{(1 - \omega/\Omega_{cH})^{3/2}}. \quad (32)$$

We consider 5 MeV electrons (a typical energy for resonant interaction with EMIC waves, see Refs. 58 and 59),  $\omega_{pe}/\Omega_{c0} \approx 15$  (EMIC waves are generally observed in the regions with enhanced plasma density<sup>33</sup>), wave amplitude is about 1 nT (see statistics in Ref. 43), and  $L = 5$ . In the presence of additional magnetic field fluctuations in the same frequency range as EMIC waves (i.e., with  $\tau \sim 2\pi/\omega$ ), electron trapping by EMIC waves is considerably more stable than trapping by whistler-mode waves: the amplitude  $\sqrt{\sigma}$  of the additional fluctuations must reach the same level as the EMIC wave amplitude  $B_w$  even to merely get  $K_0 = 0.2$ . Actually, the effect of such extremely low frequency magnetic field fluctuations becomes important only for EMIC waves with  $\omega/\Omega_{cH} > 0.9$  while general spacecraft statistics show that the typical frequency of EMIC waves in the magnetosphere is rather  $\omega/\Omega_{cH} \sim 0.5$  (see, e.g., Ref. 43).

However, EMIC waves are frequently observed in high density regions of the magnetosphere (like plasmaspheric plumes or just inside the plasmopause) in conjunction with whistler-mode hiss waves. The latter waves have much higher frequencies than EMIC waves, typically corresponding to  $2\pi/\tau \simeq 200\Omega_{cH}$ . Magnetic field fluctuations from such considerably higher frequency waves are expected to perturb trapping by EMIC waves much more efficiently than fluctuations in the same frequency range. As a result, strong hiss-like waves with amplitudes reaching locally  $\sim 15\%$  of EMIC wave amplitudes could significantly reduce the efficiency of trapping by intense EMIC waves (see Fig. 5 (right panel)). Recent Van Allen Probe measurements have shown that hiss amplitudes often reach  $>10\%$  of EMIC wave amplitudes during moderately disturbed geomagnetic conditions,<sup>39</sup> while intense hiss waves reaching  $\sim 0.2$  nT have been observed at high  $L$  on the duskside.<sup>42,79</sup> However, such strong hiss-like waves (or higher-frequency chorus) would be required to occur on the same magnetic field lines as the considered EMIC waves, which may not be always the case (e.g., see Ref. 86). Besides, it is worth noting that for trapping by EMIC waves, the corresponding  $v_{R0}$  is much larger

than the phase velocity of parallel hiss waves, so that  $v_{eff} \sim v_{R0}$  in this case.

#### IV. SPACECRAFT OBSERVATIONS

To derive equations describing the effects of magnetic field fluctuations on trapped particle motion, we assume that the timescale of these fluctuations is comparable with the period of the main wave trapping the electrons. To illustrate the presence of such fluctuations in real systems, we show two examples of observations of intense whistler-mode waves (highly oblique and parallel) in the radiation belts by one of the two Van Allen Probes<sup>41</sup> spacecrafts (see Fig. 7). The top row of panels shows one example of oblique whistler-mode waves (strong parallel electric field and weak magnetic field). In this spectrum, the central peak at  $\sim 1.5$  kHz is surrounded by fluctuations (for instance at  $\sim 1.8$  kHz or  $\sim 3$  kHz) with a magnetic field power two-three orders of magnitude smaller than the main wave intensity. Magnetic field data show that the wave amplitude reaches  $\sim 30$  pT, while the amplitude of fluctuations is about  $\sim 1 - 2.5$  pT. Figure 5 (central panel) shows that such fluctuations can significantly influence the dynamics of trapped particles. In the case of the intense weakly oblique whistler wave at  $\sim 2.4$  kHz shown in bottom panels of Fig. 7, the intensity of nearby magnetic field fluctuations is also significant. The main wave amplitude is about  $\sim 250$  pT, while surrounding fluctuations (at  $\sim 1.7$  kHz or  $\sim 3.9$  kHz) have amplitudes  $\sim 2 - 8$  pT. The latter level of fluctuations is high enough to result in particle escape from the resonance (see Fig. 5 (left panel)). Therefore, we can conclude that the effects discussed in our paper can actually occur under realistic conditions in the Earth's radiation belts.

#### V. ALTERNATIVE MECHANISMS OF DESTRUCTION OF TRAPPING MOTION

In the present study, the destruction of trapped particle motion is due to external, non-resonant magnetic field fluctuations, included as externally driven variations of the main system parameters. However, there are two other important sources of similar variations.

##### A. Modulation of wave amplitude

Intense whistler waves are usually propagating in the form of relatively long wave packets often exhibiting a fine subpacket structure corresponding to fast modulations of the wave amplitude.<sup>2,31,73,77,84</sup> For resonant whistler-mode waves with  $\theta = 0^\circ$ , these modulations concern the wave magnetic field component transverse to the geomagnetic field line, while, in the case of very oblique quasi-electrostatic whistlers, they concern the wave electric field parallel component. Such fast modulations can effectively reduce the timespan of charged particle trapped motion<sup>72,73</sup> and may be considered as fluctuations of the parameter  $\varepsilon$ . In this case, the second term in the Hamiltonian (7) can be divided into nonperturbed ( $\varepsilon w^2 \cos \phi$ ) and perturbed ( $\delta \varepsilon w^2 \cos \phi$ ) parts. The corresponding change of invariant  $I$  over one time step ( $\sim \tau \ll 2\pi/\Omega_{tr}$ ) can be written (in analogy with Eq. (11)) as

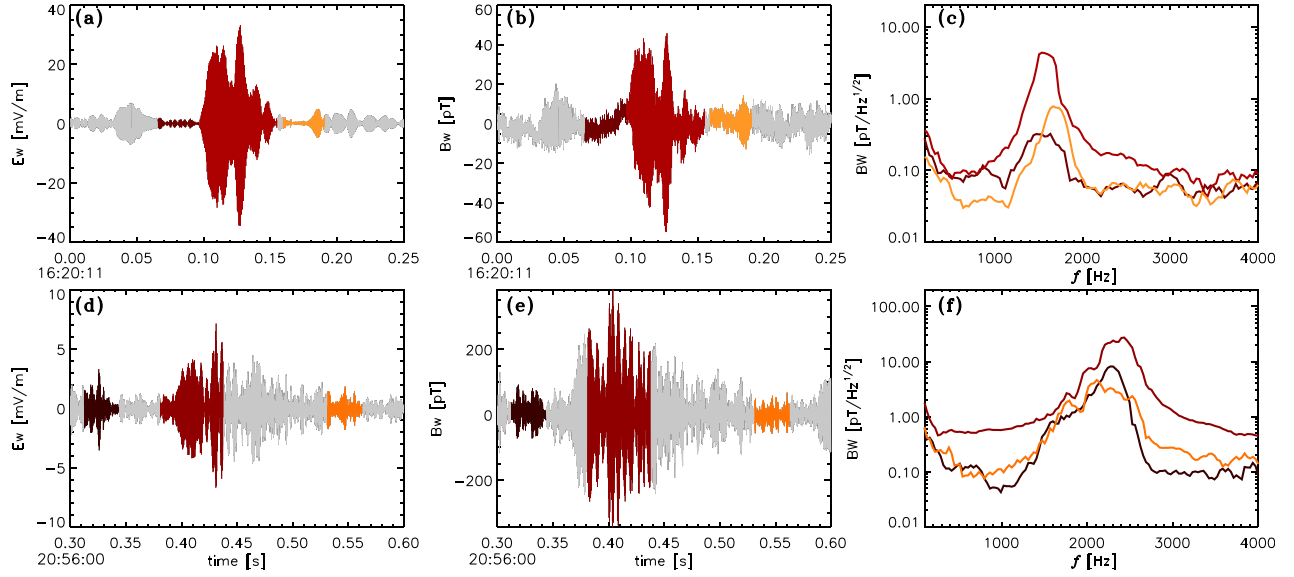


FIG. 7. The data are captured on November 1, 2012 by one Van Allen Probes spacecraft.<sup>41</sup> Electric and magnetic field waveforms were produced by the EFW<sup>85</sup> and EMFISIS<sup>34</sup> detectors. The top panels show a very oblique wave with  $\theta \sim 70^\circ$ . The bottom panels present waves with  $\theta \leq 10^\circ$ . Left panels show the parallel (relative to the background magnetic field) electric field component. Middle panels present one of the transverse components of wave magnetic field. Spectra for the intervals indicated by colors are displayed in the right panels.

$$\Delta I = \frac{1}{\Omega_{tr} g} \Delta H = \frac{1}{g} \Omega_{tr} \frac{\delta \varepsilon}{\varepsilon} \sin \phi \Delta \phi. \quad (33)$$

For  $\text{Var}(\Delta I)$ , we obtain (see Eqs. (12)–(15))

$$\text{Var}(\Delta I) \sim \Omega_{tr}^3 I \tau^2 \sigma_\varepsilon / 2, \quad (34)$$

where  $\sigma_\varepsilon = \text{Var}(\delta \varepsilon / \varepsilon)$  and  $\text{Var}(\sin \phi) = 1/2$ . Thus, the corresponding parameter  $K_0$  is

$$K_0 \approx \frac{\pi \Omega_{tr}^2 \tau R_0}{v_{R0}} \sigma_\varepsilon = \frac{\pi \varepsilon c}{v_{R0}} \Omega_{c0} \tau \sigma_\varepsilon. \quad (35)$$

Equation (35) shows that the trapped particle motion is more unstable for high wave amplitude and a larger timescale of fluctuations  $\tau$ . Thus, for charged particle trapping by very intense waves, the effect of strong modulations of the main wave amplitude can be more dangerous than the essentially diffusive effects of additional non-resonant magnetic field fluctuations studied in Section III.

## B. Externally driven pitch-angle diffusion

The term  $a$  in the Hamiltonian (5) depends on the magnetic moment  $\mu$  of trapped particles. In the case of Landau resonance,  $\mu$  is conserved, while particle trapping into cyclotron resonance results in a variation of  $\mu$  with  $s$  (for details, see Ref. 62). Thus, externally driven fluctuations of  $\mu$  should result in high-frequency variations of the term  $a$ , with a final effect similar to the effect of magnetic field fluctuations. Thus, the term  $a \sim \mu$  can be separated into two parts: undisturbed  $a_0$  and fluctuating  $a_1 = a_0(\delta \mu / \mu)$ . In this case, the main equations coincide with equations derived for fluctuations of the magnetic field, while the dimensionless variable  $K$  from Eq. (20) takes the form

$$K = \frac{2\pi \omega_*^4 R_0 \tau}{\Omega_{tr}^2 v_{R0}} \sigma_\mu \frac{w(s)}{a_0^2(s)} \int \frac{a_0^2(s') ds'}{w(s') u_R(s')}, \quad (36)$$

with  $\sigma_\mu = \text{Var}(\delta \mu / \mu)$  and  $\tau$  the timescale of  $\mu$  variations, giving

$$K_0 = \frac{2\pi c}{\varepsilon v_{R0}} \Omega_{c0} \tau \sigma_\mu. \quad (37)$$

Equation (37) provides an estimate of the role of external pitch-angle (or magnetic moment) diffusion. However, the quasi-linear pitch-angle diffusion induced by a wide spectrum of low amplitude whistler-mode waves seems to be insufficiently strong (even for highly oblique waves<sup>44</sup>) to produce a measurable change in the pitch-angle of particles within one bounce period of energetic electrons between their mirror points.<sup>45,66</sup> Nevertheless, small-scale intense electrostatic structures recently observed in the radiation belts<sup>40,46</sup> could bring forth a much more efficient pitch-angle scattering. Being generated in the form of wide packets with wide frequency ranges, these structures could interact with  $<20$  keV electrons<sup>47</sup> and the corresponding pitch-angle diffusion could result in a destruction of trapped motion. Moreover, disturbances to the current of thermal electrons caused by such electrostatic structures often generate magnetic field perturbations,<sup>83</sup> which could serve as a source for some of the magnetic field fluctuations considered in Section III.

## VI. CONCLUSIONS

In this paper, we have proposed an approach allowing to estimate the effect of additional non-resonant magnetic field fluctuations on the motion of relativistic electrons trapped by intense waves. Such an approach is principally based on the consideration of trapped electron oscillations in the phase

plane where a corresponding adiabatic invariant can be introduced. Magnetic field fluctuations can break the conservation of this invariant and ultimately result in electron detrapping. This general approach has been used here to estimate the stability of trapped motion in three systems describing electron acceleration in the Earth's radiation belts.

We show that the first and second systems describe electron trapping into the first cyclotron and Landau resonances by intense parallel and oblique whistler-mode waves. For typical wave amplitudes ( $\sim 0.1 - 1$  nT or  $\sim 10 - 100$  mV/m), additional magnetic field fluctuations with an intensity  $\sim 1 - 100$  pT<sup>2</sup> can significantly disrupt the trapped motion. The fluctuation intensity necessary for significant perturbations of the trapped motion varies with  $L$ -shell as  $\sim L^{-4}$ , and it is larger for a smaller frequency  $\omega/\Omega_{ce0}$  of the main wave.

The third system concerns electron trapping into the first cyclotron resonance by intense EMIC waves. For typical wave amplitudes  $\sim 1$  nT, significant perturbations of the trapped motion can be obtained only for much higher frequency magnetic field fluctuations at a high intensity  $\sim 10\,000$  pT<sup>2</sup>. Thus, trapped motion appears more stable than in the two previous cases. It can be perturbed only for high-frequency EMIC waves with  $\omega/\Omega_{ceH} \geq 0.5$ .

## ACKNOWLEDGMENTS

Work of A.A. was supported by Grant No. MK-1781.2014.2. Work by O.A. and F.M. was performed under JHU/APL Contract No. 922613 (RBSP-EFW). This material is based upon work supported by the National Science Foundation under Grant No. 1362782 (D.V.).

- <sup>1</sup>O. Agapitov, A. Artemyev, V. Krasnoselskikh, Y. V. Khotyaintsev, D. Mourenas, H. Breuillard, M. Balikhin, and G. Rolland, *J. Geophys. Res.* **118**, 3407–3420, doi:10.1002/jgra.50312 (2013).
- <sup>2</sup>O. Agapitov, A. Artemyev, D. Mourenas, V. Krasnoselskikh, J. Bonnell, O. Le Contel, C. M. Cully, and V. Angelopoulos, *J. Geophys. Res.* **119**, 1606–1626, doi:10.1002/2013JA019223 (2014).
- <sup>3</sup>J. M. Albert, *Phys. Fluids B* **5**, 2744–2750 (1993).
- <sup>4</sup>J. M. Albert, *J. Geophys. Res.* **105**, 21191, doi:10.1029/2000JA000008 (2000).
- <sup>5</sup>J. M. Albert and J. Bortnik, *Geophys. Res. Lett.* **36**, L12110, doi:10.1029/2009GL038904 (2009).
- <sup>6</sup>J. M. Albert, X. Tao, and J. Bortnik, “Aspects of nonlinear wave-particle interactions,” in *Dynamics of the Earth's Radiation Belts and Inner Magnetosphere*, edited by D. Summers, I. U. Mann, D. N. Baker, and M. Schulz (American Geophysical Union, 2013).
- <sup>7</sup>X. An, L. Chen, J. Bortnik, and R. M. Thorne, *J. Geophys. Res.* **119**, 1951–1959, doi:10.1002/2013JA019597 (2014).
- <sup>8</sup>V. I. Arnold, V. V. Kozlov, and A. I. Neishtadt, *Mathematical Aspects of Classical and Celestial Mechanics*, 3rd ed., Dynamical Systems III. Encyclopedia of Mathematical Sciences (Springer-Verlag, New York, 2006).
- <sup>9</sup>A. Artemyev, V. Krasnoselskikh, O. Agapitov, D. Mourenas, and G. Rolland, *Phys. Plasmas* **19**, 122901 (2012).
- <sup>10</sup>A. Artemyev, D. Vainchtein, A. Neishtadt, and L. Zelenyi, *Phys. Rev. E* **84**(4), 046213 (2011).
- <sup>11</sup>A. Artemyev, D. Vainchtein, A. Neishtadt, and L. Zelenyi, *Phys. Rev. E* **89**(4), 043106 (2014).
- <sup>12</sup>A. V. Artemyev, A. A. Vasiliev, D. Mourenas, O. Agapitov, and V. Krasnoselskikh, *Phys. Plasmas* **20**, 122901 (2013).
- <sup>13</sup>A. V. Artemyev, A. A. Vasiliev, D. Mourenas, O. Agapitov, V. Krasnoselskikh, D. Boscher, and G. Rolland, *Geophys. Res. Lett.* **41**, 5727–5733, doi:10.1002/2014GL061380 (2014).
- <sup>14</sup>A. V. Artemyev, A. A. Vasiliev, D. Mourenas, O. V. Agapitov, and V. V. Krasnoselskikh, *Phys. Plasmas* **21**(10), 102903 (2014).
- <sup>15</sup>T. F. Bell and U. S. Inan, *J. Geophys. Res.* **86**, 9047–9063, doi:10.1029/JA086iA11p09047 (1981).
- <sup>16</sup>J. Bortnik, R. M. Thorne, and U. S. Inan, *Geophys. Res. Lett.* **35**, L21102, doi:10.1029/2008GL035500 (2008).
- <sup>17</sup>A. L. Brinca, *J. Geophys. Res.* **85**, 4711–4714, doi:10.1029/JA085iA09p04711 (1980).
- <sup>18</sup>C. Cattell, J. R. Wygant, K. Goetz, K. Kersten, P. J. Kellogg, von T. Rosenvinge, S. D. Bale, I. Roth, M. Temerin, M. K. Hudson, R. A. Mewaldt, M. Wiedenbeck, M. Maksimovic, R. Ergun, M. Acuna, and C. T. Russell, *Geophys. Res. Lett.* **35**, L01105, doi:10.1029/2007GL032009 (2008).
- <sup>19</sup>C. M. Cully, J. W. Bonnell, and R. E. Ergun, *Geophys. Res. Lett.* **35**, L17S16, doi:10.1029/2008GL033643 (2008).
- <sup>20</sup>A. G. Demekhov, V. Y. Trakhtengerts, M. J. Rycroft, and D. Nunn, *Geomagn. Aeron.* **46**, 711–716, doi:10.1134/S0016793206060053 (2006).
- <sup>21</sup>A. G. Demekhov, V. Y. Trakhtengerts, M. Rycroft, and D. Nunn, *Geomagn. Aeron.* **49**, 24–29, doi:10.1134/S0016793209010034 (2009).
- <sup>22</sup>A. G. Demekhov, *Radiophys. Quantum Electron.* **53**, 609–622 (2011).
- <sup>23</sup>A. G. Demekhov and V. Y. Trakhtengerts, *Radiophys. Quantum Electron.* **51**, 880–889 (2008).
- <sup>24</sup>R. L. Dowden, *J. Geophys. Res.* **87**, 6237–6242, doi:10.1029/JA087iA08p06237 (1982).
- <sup>25</sup>N. Furuya, Y. Omura, and D. Summers, *J. Geophys. Res.* **113**, A04224, doi:10.1029/2007JA012478 (2008).
- <sup>26</sup>R. Gendrin, *Planet. Space Sci.* **5**, 274 (1961).
- <sup>27</sup>A. P. Itin, A. I. Neishtadt, and A. A. Vasiliev, *Physica D* **141**, 281–296 (2000).
- <sup>28</sup>V. I. Karpman, I. N. Istomin, and D. R. Shklyar, *Phys. Scr.* **11**, 278–284 (1975).
- <sup>29</sup>V. I. Karpman, J. N. Istomin, and D. R. Shklyar, *Plasma Phys.* **16**, 685–703 (1974).
- <sup>30</sup>V. I. Karpman and D. R. Shklyar, *Sov. Phys. JETP* **35**, 500 (1972).
- <sup>31</sup>P. J. Kellogg, C. A. Cattell, K. Goetz, S. J. Monson, and L. B. Wilson III, *Geophys. Res. Lett.* **37**, L20106, doi:10.1029/2010GL044845 (2010).
- <sup>32</sup>K. Kersten, C. A. Cattell, A. Breneman, K. Goetz, P. J. Kellogg, J. R. Wygant, L. B. Wilson III, J. B. Blake, M. D. Looper, and I. Roth, *Geophys. Res. Lett.* **38**, L08107, doi:10.1029/2011GL046810 (2011).
- <sup>33</sup>T. Kersten, R. B. Horne, S. A. Glauert, N. P. Meredith, B. J. Fraser, and R. S. Grew, *J. Geophys. Res.* **119**, 8820–8837, doi:10.1002/2014JA020366 (2014).
- <sup>34</sup>C. A. Kletzing, W. S. Kurth, M. Acuna, R. J. MacDowall, R. B. Torbert, T. Averkamp, D. Bodet, S. R. Bounds, M. Chutter, J. Connerney, D. Crawford, J. S. Dolan, R. Dvorsky, G. B. Hospodarsky, J. Howard, V. Jordanova, R. A. Johnson, D. L. Kirchner, B. Mokrzycki, G. Needell, J. Odom, D. Mark, R. Pfaff, J. R. Phillips, C. W. Piker, S. L. Remington, D. Rowland, O. Santolik, R. Schnurr, D. Sheppard, C. W. Smith, R. M. Thorne, and J. Tyler, *Space Sci. Rev.* **179**, 127–181 (2013).
- <sup>35</sup>L. D. Landau and E. M. Lifshitz, *Mechanics. Course of Theoretical Physics* (Oxford, Pergamon, 1988), Vol. 1.
- <sup>36</sup>W. Li, J. Bortnik, R. M. Thorne, and V. Angelopoulos, *J. Geophys. Res.* **116**, A12205, doi:10.1029/2011JA017035 (2011).
- <sup>37</sup>W. Li, J. Bortnik, R. M. Thorne, C. M. Cully, L. Chen, V. Angelopoulos, Y. Nishimura, J. B. Tao, J. W. Bonnell, and O. Lecontel, *J. Geophys. Res.* **118**, 1461–1471, doi:10.1002/jgra.50176 (2013).
- <sup>38</sup>K. Liu, D. Winske, S. P. Gary, and G. D. Reeves, *J. Geophys. Res.* **117**, A06218, doi:10.1029/2011JA017476 (2012).
- <sup>39</sup>Q. Ma, W. Li, R. M. Thorne, B. Ni, C. A. Kletzing, W. S. Kurth, G. B. Hospodarsky, G. D. Reeves, M. G. Henderson, H. E. Spence, D. N. Baker, J. B. Blake, J. F. Fennell, S. G. Claudepierre, and V. Angelopoulos, *Geophys. Res. Lett.* **42**, 987–995, doi:10.1002/2014GL062977 (2015).
- <sup>40</sup>D. M. Malaspina, L. Andersson, R. E. Ergun, J. R. Wygant, J. W. Bonnell, C. Kletzing, G. D. Reeves, R. M. Skoug, and B. A. Larsen, *Geophys. Res. Lett.* **41**, 5693–5701, doi:10.1002/2014GL061109 (2014).
- <sup>41</sup>B. H. Mauk, N. J. Fox, S. G. Kanekal, R. L. Kessel, D. G. Sibeck, and A. Ukhorskiy, *Space Sci. Rev.* **179**, 3–27 (2013).
- <sup>42</sup>N. P. Meredith, R. B. Horne, R. M. Thorne, D. Summers, and R. R. Anderson, *J. Geophys. Res.* **109**, A06209, doi:10.1029/2004JA010387 (2004).
- <sup>43</sup>N. P. Meredith, R. B. Horne, T. Kersten, B. J. Fraser, and R. S. Grew, *J. Geophys. Res.* **119**, 5328–5342, doi:10.1002/2014JA020064 (2014).
- <sup>44</sup>D. Mourenas, A. V. Artemyev, O. V. Agapitov, and V. Krasnoselskikh, *J. Geophys. Res.* **119**, 2775–2796, doi:10.1002/2013JA019674 (2014).
- <sup>45</sup>D. Mourenas, A. V. Artemyev, J.-F. Ripoll, O. V. Agapitov, and V. V. Krasnoselskikh, *J. Geophys. Res.* **117**, A06234, doi:10.1029/2012JA017717 (2012).

- <sup>46</sup>F. S. Mozer, S. D. Bale, J. W. Bonnell, C. C. Chaston, I. Roth, and J. Wygant, *Phys. Rev. Lett.* **111**(23), 235002 (2013).
- <sup>47</sup>F. S. Mozer, O. V. Agapitov, A. Artemyev, J. Drake, V. Krasnoselskikh, S. Lejosne, and I. Vasko, *Geophys. Res. Lett.* **42**, 3627, doi:10.1002/2015GL063946 (2015).
- <sup>48</sup>A. Neishtadt, A. Vasiliev, and A. Artemyev, *Moscow Math. J.* **11**(3), 531–545 (2011).
- <sup>49</sup>Y. Nishimura, J. Bortnik, W. Li, R. M. Thorne, L. R. Lyons, V. Angelopoulos, S. B. Mende, J. W. Bonnell, O. Le Contel, C. Cully, R. Ergun, and U. Auster, *Science* **330**, 81 (2010).
- <sup>50</sup>D. Nunn, *J. Plasma Phys.* **6**, 291 (1971).
- <sup>51</sup>D. Nunn, *Planet. Space Sci.* **22**, 349–378 (1974).
- <sup>52</sup>D. Nunn, *Planet. Space Sci.* **34**, 429–451 (1986).
- <sup>53</sup>D. Nunn and Y. Omura, *J. Geophys. Res.* **120**, 2890–2911, doi:10.1002/2014JA020898 (2015).
- <sup>54</sup>Y. Omura, N. Furuya, and D. Summers, *J. Geophys. Res.* **112**, A06236, doi:10.1029/2006JA012243 (2007).
- <sup>55</sup>Y. Omura, M. Hikishima, Y. Katoh, D. Summers, and S. Yagitani, *J. Geophys. Res.* **114**, A07217, doi:10.1029/2009JA014206 (2009).
- <sup>56</sup>Y. Omura, Y. Katoh, and D. Summers, *J. Geophys. Res.* **113**, A04223, doi:10.1029/2007JA012622 (2008).
- <sup>57</sup>Y. Omura, H. Matsumoto, D. Nunn, and M. J. Rycroft, *J. Atmos. Terr. Phys.* **53**, 351–368 (1991).
- <sup>58</sup>Y. Omura and Q. Zhao, *J. Geophys. Res.* **117**, A08227, doi:10.1029/2012JA017943 (2012).
- <sup>59</sup>Y. Omura and Q. Zhao, *J. Geophys. Res.* **118**, 5008–5020, doi:10.1002/jgra.50477 (2013).
- <sup>60</sup>M. Schulz and L. J. Lanzerotti, *Particle Diffusion in the Radiation Belts* (Springer, New York, 1974).
- <sup>61</sup>B. W. Sheeley, M. B. Moldwin, H. K. Rassoul, and R. R. Anderson, *J. Geophys. Res.* **106**, 25631–25642, doi:10.1029/2000JA000286 (2001).
- <sup>62</sup>D. Shklyar and H. Matsumoto, *Surv. Geophys.* **30**, 55–104 (2009).
- <sup>63</sup>D. R. Shklyar, *Sov. Phys. JETP* **53**, 1197–1192 (1981).
- <sup>64</sup>D. R. Shklyar, *Ann. Geophys.* **29**, 1179–1188 (2011).
- <sup>65</sup>D. R. Shklyar and G. Zimbardo, *Plasma Phys. Controlled Fusion* **56**(9), 095002 (2014).
- <sup>66</sup>Y. Y. Shprits, D. A. Subbotin, N. P. Meredith, and S. R. Elkington, *J. Atmos. Sol.-Terr. Phys.* **70**, 1694–1713 (2008).
- <sup>67</sup>V. V. Solov'ev and D. R. Shklyar, *Sov. Phys. JETP* **63**, 272–277 (1986).
- <sup>68</sup>D. Summers and R. M. Thorne, *J. Geophys. Res.* **108**, 1143, doi:10.1029/2002JA009489 (2003).
- <sup>69</sup>D. Summers and Y. Omura, *Geophys. Res. Lett.* **34**, L24205, doi:10.1029/2007GL032226 (2007).
- <sup>70</sup>D. Summers, R. Tang, Y. Omura, and D.-H. Lee, *Phys. Plasmas* **20**(7), 072110 (2013).
- <sup>71</sup>X. Tao and J. Bortnik, *Nonlinear Process. Geophys.* **17**, 599–604 (2010).
- <sup>72</sup>X. Tao, J. Bortnik, R. M. Thorne, J. M. Albert, and W. Li, *Geophys. Res. Lett.* **39**, L06102, doi:10.1029/2012GL051202 (2012).
- <sup>73</sup>X. Tao, J. Bortnik, R. M. Thorne, J. M. Albert, and W. Li, *J. Atmos. Sol.-Terr. Phys.* **99**, 67–72 (2013).
- <sup>74</sup>U. Taubenschuss, Y. V. Khotyaintsev, O. Santolík, A. Vaivads, C. M. Cully, O. L. Contel, and V. Angelopoulos, *J. Geophys. Res.* **119**, 9567–9578, doi:10.1002/2014JA020575 (2014).
- <sup>75</sup>R. M. Thorne and C. F. Kennel, *J. Geophys. Res.* **76**, 4446, doi:10.1029/JA076i019p04446 (1971).
- <sup>76</sup>V. Y. Trakhtengerts and M. J. Rycroft, *Whistler and Alfvén Mode Cyclotron Masers in Space* (Cambridge University Press, 2008).
- <sup>77</sup>B. T. Tsurutani, B. J. Falkowski, O. P. Verkhoglyadova, J. S. Pickett, O. Santolík, and G. S. Lakhina, *J. Geophys. Res.* **116**, A09210, doi:10.1029/2010JA016237 (2011).
- <sup>78</sup>B. T. Tsurutani, G. S. Lakhina, and O. P. Verkhoglyadova, *J. Geophys. Res.* **118**, 2296–2312, doi:10.1002/jgra.50264 (2013).
- <sup>79</sup>B. T. Tsurutani, B. J. Falkowski, J. S. Pickett, O. Santolík, and G. S. Lakhina, *J. Geophys. Res.* **120**, 414–431, doi:10.1002/2014JA020518 (2015).
- <sup>80</sup>A. Y. Ukhorskiy and M. I. Sitnov, *Space Sci. Rev.* **179**, 545–578 (2013).
- <sup>81</sup>M. E. Usanova, I. R. Mann, J. Bortnik, L. Shao, and V. Angelopoulos, *J. Geophys. Res.* **117**, A10218, doi:10.1029/2012JA018049 (2012).
- <sup>82</sup>D. Vainchtein and I. Mezić, *Phys. Rev. Lett.* **93**(8), 084301 (2004).
- <sup>83</sup>I. Y. Vasko, O. V. Agapitov, F. Mozer, A. V. Artemyev, and D. Jovanovic, *Geophys. Res. Lett.* **42**, 2123–2129, doi:10.1002/2015GL063370 (2015).
- <sup>84</sup>L. B. Wilson III, C. A. Cattell, P. J. Kellogg, J. R. Wygant, K. Goetz, A. Breneman, and K. Kersten, *Geophys. Res. Lett.* **38**, L17107, doi:10.1029/2011GL048671 (2011).
- <sup>85</sup>J. R. Wygant, J. W. Bonnell, K. Goetz, R. E. Ergun, F. S. Mozer, S. D. Bale, M. Ludlam, P. Turin, P. R. Harvey, R. Hochmann, K. Harps, G. Dalton, J. McCauley, W. Rachelson, D. Gordon, B. Donakowski, C. Shultz, C. Smith, M. Diaz-Aguado, J. Fischer, S. Heavner, P. Berg, D. M. Malaspina, M. K. Bolton, M. Hudson, R. J. Strangeway, D. N. Baker, X. Li, J. Albert, J. C. Foster, C. C. Chaston, I. Mann, E. Donovan, C. M. Cully, C. A. Cattell, V. Krasnoselskikh, K. Kersten, A. Breneman, and J. B. Tao, *Space Sci. Rev.* **179**, 183–220 (2013).
- <sup>86</sup>Z. Yuan, Y. Xiong, Y. Pang, M. Zhou, X. Deng, J. G. Trotignon, E. Lucek, and J. Wang, *J. Geophys. Res.* **117**, A03205, doi:10.1029/2011JA017152 (2012).
- <sup>87</sup>A. Zaslavsky, C. Krafft, L. Gorbunov, and A. Volokitin, *Phys. Rev. E* **77**, 056407 (2008).